Space-Time-Multipath Coding Using Digital Phase Sweeping or Circular Delay Diversity

Xiaoli Ma, *Member, IEEE,* and Georgios B. Giannakis, *Fellow, IEEE*

***Abstract*—We design novel space-time multipath (STM) coded multi-antenna transmissions over frequency-selective Rayleigh fading channels. We develop STM coded systems that guarantee the maximum possible space-multipath diversity, along with large coding gains, and high bandwidth efficiency for any number of transmit-receive antennas. By incorporating subchannel grouping, we also enable desirable tradeoffs between performance and complexity. Our designs rely on digital phase sweeping or block circular delay operations and apply to both single- and multi-carrier systems. Their merits are confirmed by corroborating simulations and comparisons with existing approaches.**

***Index Terms*—Coding, diversity, frequency-selective fading, multi-carrier transmission, phase sweeping.**

I. Introduction

BROADBAND wireless communications call for high data rates and high performance. As high rates imply reduced symbol duration relative to the channel delay spread, frequency-selective propagation effects become more pronounced. Therefore, it is important for broadband wireless applications to design single- or multi-antenna systems that account for (and if possible exploit) frequency-selective multipath fading.

Space-time (ST) coding has been proved effective in combating fading and enhancing data rates. Taking advantage of the *space* diversity offered by multiple transmit (and possibly multiple receive) antennas, ST-coded transmissions over flat fading channels have well documented merits; see, e.g., [16] and [17]. Frequency-selective channels, on the other hand, provide *multipath* diversity [21]. Multi-antenna transmissions over frequency-selective channels have thus the potential to achieve joint space-multipath diversity [12], [13], [24]. ST coding for frequency-selective channels has been pursued recently both for single-carrier [2], [10], [11], [19], [24], as well as for multi-carrier transmissions [3], [4], [12], [13]. Specifically, [1], [3], and [13] adopt the trellis coded modulation (TCM) codes of [16], without full space-multipath diversity gain guarantees, while [4] enables the maximum diversity gains at the expense of bandwidth efficiency. The ST designs in [12] and [24] (which also subsumes [2], [10], and [19]) guarantee full diversity, but as they rely on the ST block codes of [17], they incur rate loss up to 50%, when the number of transmit antennas $N_t > 2$ and complex constellations are used. In fact, all schemes relying on the orthogonal ST block codes of [17] suffer from this inherent rate limitation. ST trellis codes do not necessarily incur rate loss [16]. However, as N_t increases, designing ST trellis codes to guarantee certain diversity and coding gains becomes increasingly difficult.

Delay diversity schemes offer a simpler design option. They were originally developed for flat-fading channels [15], but they have been extended recently to frequency-selective ones by transmitting one symbol over two antennas in different time-slots [5], [14], [15]. Similarly, a so-termed phase sweeping transmission that creates time-variations to an originally slow-fading channel was introduced in [6]. Unfortunately, existing *analog* phase-sweeping and delay-diversity approaches [5], [6], [14], [15] consume extra bandwidth, and they do not enable joint space-multipath diversity gains.

Starting from a multi-antenna OFDM transmission, we develop in this paper a multi-carrier space-time multipath (STM) coded system, which guarantees full space-multipath diversity and large coding gains with high bandwidth efficiency for *any* number of transmit antennas. Our STM codec comprises a properly designed *digital* phase-sweeping (DPS) scheme. Unlike [6] and [8], DPS renders the set of frequency-selective fading channels equivalent to a single channel. Furthermore, we show that our DPS design is equivalent to a *block circular-delay* (BCD) design. Our DPS and BCD designs do not consume extra bandwidth. Combined with the subcarrier grouping method [12], [20], our STM codec is also flexible to tradeoff desirable performance for affordable decoding complexity.

The rest of the paper is organized as follows. Section II introduces a general linearly coded system model and derives performance criteria for STM coding. Section III deals with our STM encoder and decoder. The performance of STM is analyzed in Section IV. Section V shows why our STM design amounts to circular delay diversity and describes single-carrier extensions. Section VI verifies our STM performance claims by simulations, and Section VII concludes this paper.

Notation: Upper (lower) bold face letters will be used for matrices (column vectors). Superscript $^{\mathcal{H}}$ will denote Hermitian, * conjugate, ^{T} transpose, and † pseudo-inverse. We will reserve $\otimes$ for the Kronecker product and $\mathrm{E}[\cdot]$ for expectation. We will use $[\mathbf{A}]_{k,m}$ to denote the $(k+1, m+1)$st entry of a matrix $\mathbf{A}$, $\mathrm{tr}(\boldsymbol{A})$ for its trace, and $[\mathbf{x}]_m$ to denote the $(m+1)$st entry of the

Manuscript received September 25, 2003; revised March 5, 2004. This work was supported by the Communications and Networks Consortium sponsored by the U. S. Army Research Laboratory under the Collaborative Technology Alliance Program, Cooperative Agreement DAAD19-01-2-0011. The U. S. Government is authorized to reproduce and distribute reprints for Government purposes notwithstanding any copyright notation thereon. This paper was presented in part at the GLOBECOM Conference, Taipei, Taiwan, R.O.C., November 17–21, 2002. The associate editor coordinating the review of this manuscript and approving it for publication was Prof. Zhi Ding.

X. Ma is with the Department of Electrical and Computer Engineering, Auburn University, AL 36849 USA (e-mail: xiaoli@eng.auburn.edu).

G. B. Giannakis is with the Department of Electrical and Computer Engineering, University of Minnesota, Minneapolis, MN 55455 USA (e-mail: georgios@ece.umn.edu).

Digital Object Identifier 10.1109/TSP.2004.842194

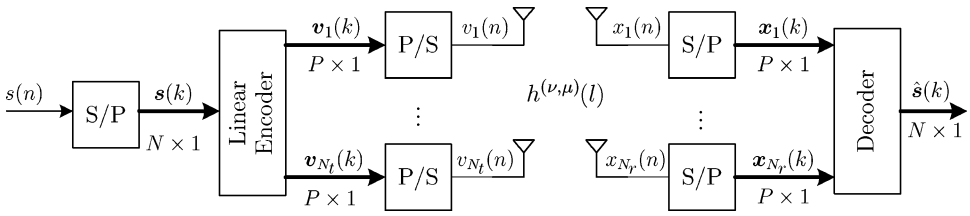

Fig. 1. Discrete-time Tx-Rx model of linearly coded ST designs.

column vector $\mathbf{x}$; $\boldsymbol{I}_N$ will denote the $N \times N$ identity matrix and $\boldsymbol{F}_N$ the $N \times N$ normalized (unitary) FFT matrix; diag$[\boldsymbol{x}]$ will stand for a diagonal matrix with $\boldsymbol{x}$ on its main diagonal.

II. Preliminaries

A. System Model

Fig. 1 depicts the discrete-time baseband equivalent model of a multi-antenna wireless system with N_t transmit and N_r receive antennas. The information bearing symbols $\{s(n)\}$ are drawn from a finite alphabet $\mathcal{A}_s$ and are parsed into blocks of size $N \times 1$. Since, in the following, we consider block-by-block transmissions, without loss of generality, we take one block: $\boldsymbol{s} := [s(0), \ldots, s(N-1)]^T$. The linear encoder in Fig. 1 maps $\boldsymbol{s}(k)$ to a codeword

$$\boldsymbol{v}_\mu = \sum_{n=0}^{N-1} \boldsymbol{a}_n^{(\mu)} [\boldsymbol{s}]_n + \boldsymbol{b}_n^{(\mu)} [\boldsymbol{s}]_n^*, \quad \forall \mu \in [1, N_t] \tag{1}$$

where $\boldsymbol{a}_n^{(\mu)}$ and $\boldsymbol{b}_n^{(\mu)}$ are $P \times 1$ vectors. As symbols and their complex conjugates are linearly combined to form the codeword $\boldsymbol{v}_\mu$ transmitted from the μth antenna during each block interval, we call the mapping in (1) a *linear ST coder*. The fading channel between the μth transmit and the νth receive antenna is assumed to be frequency-selective. The sampled baseband equivalent impulse response vector (that includes transmit and receive filters) is given by $\boldsymbol{h}^{(\nu,\mu)} := [h^{(\nu,\mu)}(0), \ldots, h^{(\nu,\mu)}(L)]^T$, $L := \lfloor \tau_{\max}/T_s \rfloor$, where $\tau_{\max}$ is the maximum delay among all paths (delay spread), T_s is the symbol (equal to the sampling) period, and L denotes the maximum order of all (ν, μ) channels. We assume ideal carrier synchronization, timing, and symbol-rate sampling. At the νth receive antenna, the symbol rate sampled sequence $x_\nu(n)$ at the receive-filter output is

$$x_\nu(n) = \sum_{\mu=1}^{N_t} \sum_{l=0}^{L} h^{(\nu,\mu)}(l) v_\mu(n-l) + \zeta_\nu(n) \tag{2}$$

where $v_\mu(n) := [\boldsymbol{v}_\mu]_n$, and $\zeta_\nu(n)$ is complex additive white Gaussian noise (AWGN) with mean zero and variance $\sigma_\zeta^2 = N_0$.

The symbols $x_\nu(n)$ are serial-to-parallel (S/P) converted to form $P \times 1$ blocks $\boldsymbol{x}_\nu := [x_\nu(0), \ldots, x_\nu(P-1)]^T$. The matrix-vector counter part of (2) is

$$\boldsymbol{x}_\nu = \sum_{\mu=1}^{N_t} \left(\boldsymbol{H}^{(\nu,\mu)} \boldsymbol{v}_\mu + \boldsymbol{H}_{ibi}^{(\nu,\mu)} \boldsymbol{v}_\mu^{ibi} \right) + \boldsymbol{\zeta}_\nu \tag{3}$$

where $\boldsymbol{H}^{(\nu,\mu)}$ is a lower triangular Toeplitz matrix with entries $[\boldsymbol{H}^{(\nu,\mu)}]_{m,n} = h^{(\nu,\mu)}(m-n)$, $\boldsymbol{H}_{ibi}^{(\nu,\mu)}$ is an upper triangular Toeplitz matrix with entries $[\boldsymbol{H}_{ibi}^{(\nu,\mu)}]_{m,n} = h^{(\nu,\mu)}(m-n+P)$, $\boldsymbol{v}_\mu^{ibi}$ is the interblock interference from the previous block, and $\boldsymbol{\zeta}_\nu$ is the AWGN vector.

Our *goal* is to develop a linearly ST-coded system capable of collecting the maximum joint space-multipath diversity as well as large coding gains with high bandwidth efficiency $\forall N_t \geq 2$.

B. Design Criteria

We will first introduce criteria for designing our STM codes based on the following assumptions.

- A1) Channel taps $\{h^{(\nu,\mu)}(l)\}_{l=0}^{L}$ are zero-mean, complex Gaussian random variables.
- A2) Channel state information (CSI) is available at the receiver but unknown to the transmitter.
- A3) High SNR is considered for deriving the STM diversity and coding gains.

When transmissions experience rich scattering, and no line-of-sight is present, the central limit theorem validates A1). Notice that we allow not only for independent random channel coefficients but also for correlated ones. A2) motivates the use of ST coding altogether. A3) will be used for asserting optimality of our designs, but it will not be required for the system operation.

Since our design will allow for correlated channels, we will denote the $N_t N_r (L+1) \times N_t N_r (L+1)$ channel correlation matrix and its rank, respectively, by

$$\boldsymbol{R}_h := \mathrm{E}[\boldsymbol{h}\boldsymbol{h}^{\mathcal{H}}], \text{ and } r_h := \mathrm{rank}(\boldsymbol{R}_h) \leq N_t N_r (L+1) \tag{4}$$

where the $N_t N_r (L+1) \times 1$ channel vector is $\boldsymbol{h} := [h^{(1,1)}(0), \ldots, h^{(1,1)}(L), \ldots, h^{(1,N_t)}(L), \ldots, h^{(N_r,N_t)}(L)]^T$. With these definitions, we can summarize our performance results for the linearly coded systems as follows (see Appendix A for a proof).

Proposition 1: At high SNR, the maximum space-multipath diversity order achieved by maximum likelihood (ML) decoding any linearly coded ST transmission through frequency-selective channels of order L is

$$G_d^{\max} = r_h \leq N_t N_r (L+1). \tag{5}$$

When $\boldsymbol{R}_h$ has full rank, the maximum coding gain for any linearly ST-coded system is

$$G_c^{\max} = (\det(\boldsymbol{R}_h))^{\frac{1}{r_h}} \frac{d_{\min}^2}{N_t} \tag{6}$$

where $d_{\min}$ is the minimum Euclidean distance of the constellation points in the finite alphabet $\mathcal{A}_s$.

The space-multipath diversity order of multi-antenna transmissions over frequency-selective channels has also been derived in [12], [13], and [24]. The novelty of Proposition 1 is threefold.

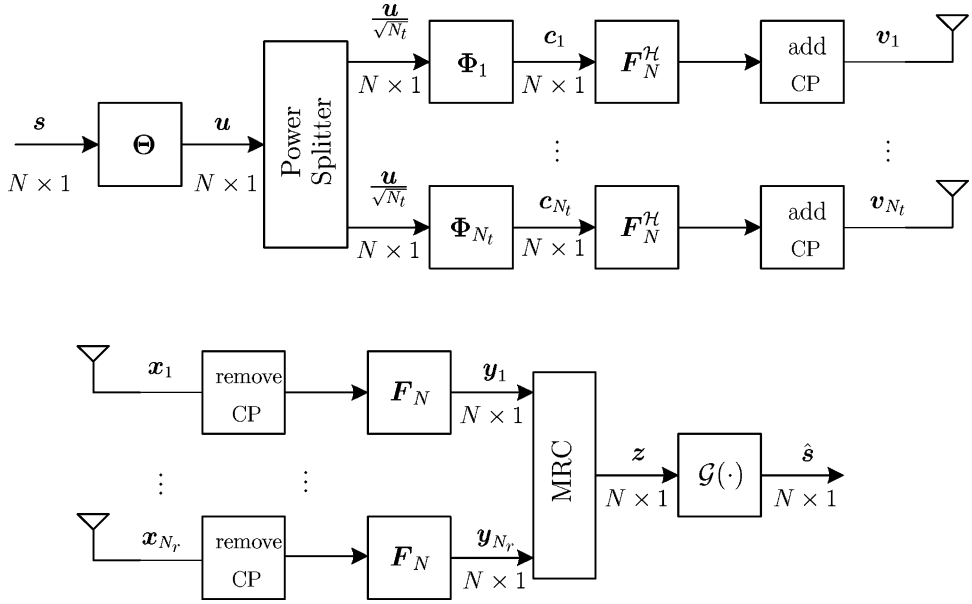

Fig. 2. Discrete-time Tx-Rx model of DPS-based STM designs.

a) It quantifies the diversity order $G_d^{\max}$ for any linearly coded ST system and can, in fact, be generalized to also include Galois–Field coded symbols.
b) It derives in closed-form the maximum coding gain $G_c^{\max}$ of all linearly coded ST transmissions.
c) It allows for correlated channels, which is important since practical frequency-selective channels are correlated with an exponential power profile.

Together, $G_d^{\max}$ and $G_c^{\max}$ offer valuable performance metrics to benchmark all linearly coded ST systems. In the ensuing section, we will derive our STM design that guarantees $G_d^{\max}$ in (29) and approaches $G_c^{\max}$ in (6) as N increases. Compared with [12] and [24], a distinct feature of our STM design here is that no rate loss is incurred $\forall N_t > 2$.

III. STM Codec Design

At a high-level view, our STM system consists of three stages, as shown in Fig. 2. The *outer codec* includes a linear constellation precoding (LCP) matrix $\boldsymbol{\Theta}$ and the corresponding deprecoder $\mathcal{G}(\cdot)$. The *middle codec* implements a digital phase sweeping (DPS) operation. It includes a power splitter along with a set of matrices $\{\boldsymbol{\Phi}_\mu\}_{\mu=1}^{N_t}$ at the transmitter and a maximum ratio combiner (MRC) at the receiver. The *inner codec* performs orthogonal frequency division multiplexing (OFDM). In the following, we will detail these three stages, starting with inner stage.

A. Inner Codec: OFDM

At the transmitter, the inner encoder comprises an OFDM module performing inverse fast Fourier transform (IFFT) operation (via the matrix $\boldsymbol{F}_N^{\mathcal{H}}$), followed by cyclic-prefix (CP) insertion. At the receiver, the inner decoder performs two mirror operations: The CP is removed, and the FFT is taken. It is well known that by (inserting) removing the CP and (I)FFT processing, a frequency-selective channel becomes equivalent to a set of flat-fading subchannels. Based on these steps, the input–output relationship from $\boldsymbol{c}_\mu$ to $\boldsymbol{y}_\nu$ (see Fig. 2) can be expressed as

$$\boldsymbol{y}_\nu = \rho \sum_{\mu=1}^{N_t} \boldsymbol{D}_H^{(\nu,\mu)} \boldsymbol{c}_\mu + \boldsymbol{\xi}_\nu, \quad \forall \nu \in [1, N_r] \tag{7}$$

where $\rho := \sqrt{N/(N+L_{cp})}$ is a power-normalizing constant accounting for the CP length L_{cp}; the $\boldsymbol{\xi}_\nu$'s are independent identically distributed (i.i.d.) AWGN vectors, $\boldsymbol{c}_\mu$ is the output of the middle encoder $\boldsymbol{\Phi}_\mu$, and $\boldsymbol{D}_H^{(\nu,\mu)} := \text{diag}[H^{(\nu,\mu)}(0), \ldots, H^{(\nu,\mu)}(N-1)]$, with $H^{(\nu,\mu)}(n) := \sum_{l=0}^{L} h^{(\nu,\mu)}(l) e^{-j2\pi nl/N}$. Comparing (7) with (3), we confirm that the inner codec (OFDM) removes the interblock interference (IBI) and diagonalizes the channel matrices.

B. Middle Codec: DPS

The middle encoder relies on the phase sweeping idea (a.k.a., intentional frequency offset [8]), which was introduced in [6]. In the two transmit-antenna *analog* implementation of [6], the signal of one antenna is modulated by a sweeping frequency f_s in addition to the carrier frequency $f_c \gg f_s$ that is present in both antennas. This causes bandwidth expansion by f_s Hz. In the following, we will derive a *digital* phase sweeping (DPS) encoder. Combined with OFDM, DPS will convert N_t frequency-selective channels, each having $(L+1)$ taps, to a single longer frequency-selective channel with $N_t(L+1)$ taps. Toward this objective, let us rewrite the diagonal channel matrix as

$$\boldsymbol{D}^{(\nu,\mu)} = \sum_{l=0}^{L} h^{(\nu,\mu)}(l) \boldsymbol{D}_l, \quad \forall \nu \in [1, N_r] \tag{8}$$

where $\boldsymbol{D}_l := \text{diag}[1, \exp(-j2\pi l/N), \ldots, \exp(-j2\pi l(N-1)/N)]$. Equation (8) discloses that different channels may have different channel taps $h^{(\nu,\mu)}(l)$, but they all share common delay lags (l) that manifest themselves as common shifts in the FFT domain. Suppose that we shift the $L+1$ taps of each channel corresponding to one of the N_t transmit antennas so that all channel taps become consecutive in their delay lags.

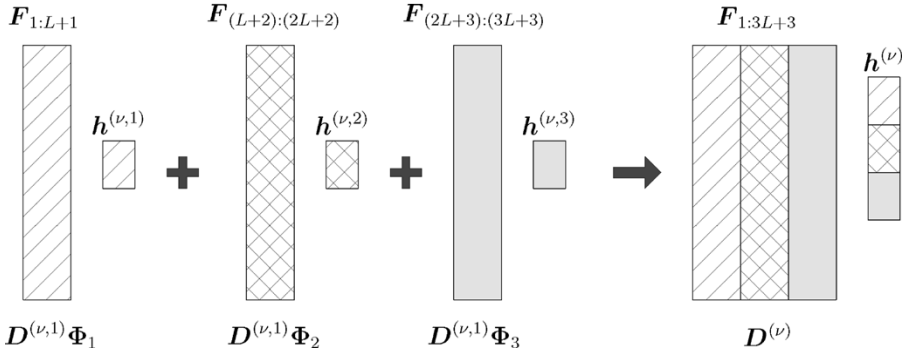

Fig. 3. Three channels are equivalent to one longer channel.

Then, we can view the N_t channels to each receive antenna as one longer frequency-selective channel with $N_t(L+1)$ taps. To realize this idea digitally, we select matrices

$$\boldsymbol{\Phi}_\mu = \text{diag}\left[1, e^{j\phi_\mu}, \ldots, e^{j\phi_\mu(N-1)}\right], \quad \forall \mu \in [1, N_t] \tag{9}$$

where $\phi_\mu = -2\pi(\mu-1)(L+1)/N$. Based on (8) and (9), we can easily verify that

$$\boldsymbol{D}_l\boldsymbol{\Phi}_\mu = \boldsymbol{D}_{l+(\mu-1)(L+1)}, \quad \forall l \in [0, L], \mu \in [1, N_t]. \tag{10}$$

Let us now define the equivalent longer channel vector corresponding to the νth receive antenna as $\boldsymbol{h}^{(\nu)} = [(\boldsymbol{h}^{(\nu,1)})^T, \ldots, (\boldsymbol{h}^{(\nu,N_t)})^T]^T$, with the lth entry of $\boldsymbol{h}^{(\nu)}$ given by $h^{(\nu)}(l) = h^{(\nu,\lfloor l/(L+1)\rfloor+1)}(l \bmod (L+1))$. Since $\boldsymbol{h}^{(\nu)}$ has length $N_t(L+1)$, we can view it as coming from a single frequency-selective channel. According to (10), let us also define the diagonal matrix of this longer equivalent channel as

$$\boldsymbol{D}_H^{(\nu)} := \sum_{\mu=1}^{N_t} \boldsymbol{D}_H^{(\nu,\mu)}\boldsymbol{\Phi}_\mu = \sum_{l=0}^{N_t(L+1)-1} h^{(\nu)}(l)\boldsymbol{D}_l. \tag{11}$$

In essence, the DPS matrix $\boldsymbol{\Phi}_\mu$ shifts the delay lags of the μth channel (c.f. (10)) from $[0, L]$ to $[(\mu-1)(L+1), \mu(L+1)-1]$. For example, when $\mu = 1$, $\boldsymbol{\Phi}_1 = \boldsymbol{I}_N$, and then, $\boldsymbol{D}^{(\nu,1)}\boldsymbol{\Phi}_1 = \text{diag}(\sqrt{N}\boldsymbol{F}_{0:L}\boldsymbol{h}^{(\nu,1)})$, where $\boldsymbol{F}_{0:L}$ denotes the first $L+1$ columns of $\boldsymbol{F}_N$. When $\mu = 2$, $\boldsymbol{D}^{(\nu,2)}\boldsymbol{\Phi}_2 = \text{diag}(\sqrt{N}\boldsymbol{F}_{(L+1):(2L+1)}\boldsymbol{h}^{(\nu,2)})$, where $\boldsymbol{F}_{(L+1):(2L+1)}$ denotes the $(L+1)$st up to $(2L+1)$st columns of $\boldsymbol{F}_N$. Proceeding likewise with all N_t DPS matrices (see Fig. 3), we can also obtain (11). We summarize this observation in the following.

Property 1: DPS converts the N_t transmit-antenna system, where each frequency-selective channel has $L+1$ taps, to a single transmit-antenna system, where the equivalent channel has $N_t(L+1)$ taps.

Equation (11) and Fig. 3 hint toward a possible relationship between our DPS codec and the delay diversity schemes of [5] and [14]. We will elaborate further on this in Section V.

Remark 1: To avoid overlapping the shifted bases, we should make sure that our block size $N > N_t(L+1)$. From the definition of the channel order $L := \lfloor \tau_{\max}/T_s \rfloor$, we have that for fixed $\tau_{\max}$ and N, we can adjust the sampling period T_s to satisfy this condition, or equivalently, for fixed T_s and $\tau_{\max}$, we can adjust the block size N. Since, for each receive antenna, we have $N_t(L+1)$ unknown channel taps corresponding to N_t channels every N symbols, this condition guarantees that the number of unknowns is less than the number of equations. Therefore, this condition is reasonable, even from a channel estimation point of view.

Using the DPS matrices (9), we will normalize (power split) $\boldsymbol{\Phi}_\mu\boldsymbol{u}$ to obtain the middle encoder output $\boldsymbol{c}_\mu = \boldsymbol{\Phi}_\mu\boldsymbol{u}/\sqrt{N_t}, \forall \mu \in [1, N_t]$. The input–output relationship (7) can then be rewritten as [c.f. (11)]

$$\boldsymbol{y}_\nu = \frac{\rho}{\sqrt{N_t}}\boldsymbol{D}_H^{(\nu)}\boldsymbol{u} + \boldsymbol{\xi}_\nu, \quad \forall \nu \in [1, N_r]. \tag{12}$$

To collect the full diversity and large coding gains, we not only need to design the transmitter properly, but we must also select a proper decoder at the receiver. Since the received blocks $\boldsymbol{y}_\nu$ from all N_r receive antennas contain the information block $\boldsymbol{s}$, we need to combine the information from all received blocks to decode $\boldsymbol{s}$. To retain decoding optimality, we perform maximum ratio combining (MRC). The MRC amounts to combining $\{\boldsymbol{y}_\nu\}_{\nu=1}^{N_r}$ in (12) to form $\boldsymbol{z} = \boldsymbol{G}\boldsymbol{y}$ using the matrix

$$\boldsymbol{G} = \left(\sum_{\nu=1}^{N_r} \boldsymbol{D}_H^{(\nu)}\left(\boldsymbol{D}_H^{(\nu)}\right)^*\right)^{-\frac{1}{2}} \left[\left(\boldsymbol{D}_H^{(1)}\right)^* \ \cdots \ \left(\boldsymbol{D}_H^{(N_r)}\right)^*\right] \tag{13}$$

with $\boldsymbol{y} := [\boldsymbol{y}_1^T, \ldots, \boldsymbol{y}_{N_r}^T]^T$. Existence of the inverse in (13) requires the channels $\boldsymbol{D}_H^{(\nu)}$ to satisfy the following coprimeness condition:

A4) $\det(\sum_{\nu=1}^{N_r} \boldsymbol{D}_H^{(\nu)}(\boldsymbol{D}_H^{(\nu)})^*) \neq 0$.

Assumption A4) is more technical rather than restrictive since it requires that the equivalent channels do not have common channel nulls. Indeed, for random channels, A4) excludes an event with probability measure zero.

With the MRC of (13), the vector $\boldsymbol{z}$ is given by [c.f. (12)]:

$$\boldsymbol{z} = -\frac{\rho}{\sqrt{N_t}}\left(\sum_{\nu=1}^{N_r} \bar{\boldsymbol{D}}_H^{(\nu)}\left(\bar{\boldsymbol{D}}_H^{(\nu)}\right)^*\right)^{\frac{1}{2}}\boldsymbol{u} + \boldsymbol{\eta} \tag{14}$$

where $\boldsymbol{\eta} := \boldsymbol{G}[\boldsymbol{\zeta}_1^T, \ldots, \boldsymbol{\zeta}_{N_r}^T]^T$. Under A4), we can verify that $\boldsymbol{G}$ satisfies $\boldsymbol{G}\boldsymbol{G}^{\mathcal{H}} = \boldsymbol{I}$. Since the $\boldsymbol{\zeta}_\nu$'s are uncorrelated AWGN blocks, the noise vector $\boldsymbol{\eta}$ retains their whiteness. From (7) and (14), we deduce that the middle codec has converted a multi-input multi-output system into a single-input single-output system with longer impulse response.

To achieve full diversity, we still need to design the outer codec properly. If there is no precoding, i.e., $\boldsymbol{u} = \boldsymbol{s}$, the diversity order is one even if ML decoding is used. To enable the full

$N_t(L+1)$ space-multipath diversity established by Proposition 1, we also need to design the precoder $\boldsymbol{\Theta}$ judiciously.

C. Outer Codec: Linear Constellation Precoding

We will design $\boldsymbol{\Theta}$ using the Grouped Linear Constellation Precoding (GLCP) scheme introduced in [12] and [23]. GLCP provides a means of reducing decoding complexity without sacrificing diversity or coding gains. To apply GLCP, we select the transmitted block size $N = N_g N_{\rm sub}$ and demultiplex the information vector $\boldsymbol{s}$ into N_g groups: $\{\boldsymbol{s}_g\}_{g=0}^{N_g-1}$, with each group having length $N_{\rm sub}$, e.g., the gth group contains the symbols collected in a vector $\boldsymbol{s}_g$ as follows: $\boldsymbol{s}_g = [[\boldsymbol{s}]_{N_{\rm sub}g}, \ldots, [\boldsymbol{s}]_{N_{\rm sub}(g+1)-1}]^T, \forall g \in [0, N_g - 1]$. Correspondingly, we define the gth linearly precoded group as

$$\boldsymbol{u}_g = \boldsymbol{\Theta}_{\rm sub}\boldsymbol{s}_g, \quad \forall g \in [0, N_g - 1] \tag{15}$$

where $\boldsymbol{\Theta}_{\rm sub}$ is an $N_{\rm sub} \times N_{\rm sub}$ matrix. To enable the maximum diversity, we select $\boldsymbol{\Theta}_{\rm sub}$ from the algebraic designs of [23]. The overall transmitted block $\boldsymbol{u}$ consists of multiplexed subblocks $\{\boldsymbol{u}_g\}_{g=0}^{N_g-1}$:

$$\boldsymbol{u} = \Big[[\boldsymbol{u}_0]_0 \cdots \big[\boldsymbol{u}_{N_g-1}\big]_0 \cdots [\boldsymbol{u}_0]_{N_{\rm sub}-1} \cdots \big[\boldsymbol{u}_{N_g-1}\big]_{N_{\rm sub}-1}\Big]^T. \tag{16}$$

It is not difficult to verify that $\boldsymbol{u}$ can be obtained from $\{\boldsymbol{u}_g\}_{g=0}^{N_g-1}$'s via a block interleaver with depth $N_{\rm sub}$. Equivalently, we can also relate $\boldsymbol{u}$ to $\boldsymbol{s}$ as

$$\boldsymbol{u} = \boldsymbol{\Theta}\boldsymbol{s}, \text{ with } \boldsymbol{\Theta} := \begin{bmatrix} \boldsymbol{I}_{N_g} \otimes \boldsymbol{\theta}_1^T \\ \vdots \\ \boldsymbol{I}_{N_g} \otimes \boldsymbol{\theta}_{N_{\rm sub}}^T \end{bmatrix} \tag{17}$$

where $\boldsymbol{\theta}_m^T$ is the mth row of $\boldsymbol{\Theta}_{\rm sub}$. Equations (15) and (16), or equivalently (17), summarize how the GLCP encoder is applied to our DPS-based STM design.

To decode GLCP transmissions, we split $\boldsymbol{z}$ in (14) into N_g groups:

$$\boldsymbol{z}_g = \frac{\rho}{\sqrt{N_t}}\boldsymbol{D}_{H,g}\boldsymbol{\Theta}_{\rm sub}\boldsymbol{s}_g + \boldsymbol{\eta}_g, \quad \forall g \in [0, N_g - 1] \tag{18}$$

where $\boldsymbol{z}_g := [[\boldsymbol{z}]_g, [\boldsymbol{z}]_{N_{\rm sub}+g}, \ldots, [\boldsymbol{z}]_{N_{\rm sub}(N_g-1)+g}]^T$; $\boldsymbol{D}_{H,g}$ is the corresponding diagonal submatrix from $(\sum_{\nu=1}^{N_r} \boldsymbol{D}_H^{(\nu)} (\boldsymbol{D}_H^{(\nu)})^*)^{\frac{1}{2}}$ for the gth group, and similarly defined, $\boldsymbol{\eta}_g$ is the corresponding AWGN vector from $\boldsymbol{\eta}$. ML decoding of $\boldsymbol{z}$ can then be implemented by applying the Sphere Decoding (SD) algorithm [18] on subblocks $\boldsymbol{z}_g$ of small size $N_{\rm sub}$. Compared with the exponentially complex ML decoder, the SD offers near-ML performance at complexity of order $\mathcal{O}(N_{\rm sub}^{\alpha})$, with $\alpha \in [3, 6]$. The SD complexity depends on the block size $N_{\rm sub}$, but unlike ML, it is independent of the constellation size at least for pulse amplitude modulated and quadrature amplitude modulated constellations [18].

Before we proceed to check the performance of STM, we summarize our DPS-based STM scheme as follows:

At the transmitter, do the following:

- T1) Given N_t, N_r, and L, choose the number of groups N_g and the group size $N_{\rm sub}$ depending on affordable complexity; and select $N = N_g N_{\rm sub} > N_t(L+1)$.
- T2) Design the $N_{\rm sub} \times N_{\rm sub}$ linear constellation precoder $\boldsymbol{\Theta}_{\rm sub}$ as in [23].
- T3) Form the precoded vector $\boldsymbol{u}$ according to (15) and (16), and split the power to form $\boldsymbol{u}/\sqrt{N_t}$.
- T4) Apply DPS via $\boldsymbol{\Phi}_\mu$ to $\boldsymbol{u}$, and obtain $\boldsymbol{c}_\mu = \boldsymbol{\Phi}_\mu \boldsymbol{u}/\sqrt{N_t}$, $\forall \mu \in [1, N_t]$.
- T5) Modulate each block $\boldsymbol{c}_\mu$ using OFDM.

At the receiver, do the following:

- R1) Implement OFDM demodulation.
- R2) Perform MRC of blocks from all receive antennas as in (14).
- R3) Split the MRC output block into N_g groups.
- R4) Implement ML (or sphere) decoding for each reduced size group as in (18).

IV. Performance Analysis

In Section II, we benchmarked the performance of any linearly coded ST system with N_t transmit and N_r receive antennae. It is not difficult to verify that our STM codec design in Section III belongs to this class of linearly coded ST systems. Thus, the diversity and coding gain results for our STM can be summarized in the following proposition.

Proposition 2: The maximum achievable space-multipath diversity order $G_d^{\max} = r_h$ is guaranteed by our STM design, provided that we select $N_{\rm sub} \geq N_t(L+1)$. When the channel correlation matrix $\boldsymbol{R}_h$ has full rank $r_h = N_r N_t(L+1)$, our STM design achieves (as $\rho = \sqrt{N/(N+L_{cp})} \to 1$) the maximum possible coding gain among all linearly coded ST systems. The coding gain of our STM scheme is given in closed form by $G_c = (\det(\boldsymbol{R}_h))^{(1/r_h)} d_{\min}^2 N/(N_t(N+L_{cp}))$. The transmission rate of STM is $N/(N+L_{cp})$ symbols/s/Hz, $\forall N_t$, N_r.

Note that in order to achieve the maximum possible coding gain using STM, one needs to design $\boldsymbol{\Theta}_{\rm sub}$ carefully; in addition, the channel correlation matrix must have full rank. Notice, however, that our maximum diversity claim holds even for channels with rank-deficient correlation matrices. Our choice of the group size $N_{\rm sub}$ determines whether the maximum diversity order can be achieved. In fact, $N_{\rm sub}$ offers flexibility to tradeoff between performance and decoding complexity. When $N_{\rm sub} \leq N_t(L+1)$, as $N_{\rm sub}$ decreases, the decoding complexity decreases, while at the same time, the diversity order decreases. By adjusting $N_{\rm sub}$, we can balance the affordable complexity with the prescribed performance. This is important because for a large number of transmit-receive antennae, or large delay spreads, one does not have to strive for diversity orders greater than four (which in fact show up for unrealistically high SNRs). In such cases, small $N_{\rm sub}$ sizes (two or four) are recommended because they allow for ML decoding with reduced complexity.

Corollary 1: When $\boldsymbol{R}_h$ has full rank, i.e., $r_h = N_t N_r(L+1)$, our STM achieves diversity order $G_d = N_{\rm sub} N_r$ when $N_{\rm sub} < N_t(L+1)$ and $G_d = N_t N_r(L+1)$ when $N_{\rm sub} \geq N_t(L+1)$.

Due to space limitations, we omit the proofs for Corollary 1 and Proposition 2. Note that different from the group size of $\boldsymbol{\Theta}_{\rm sub}$ in [12], maximum diversity in STM is enabled using $N_{\rm sub} \geq N_t(L+1)$. However, for the design in [12], the size of

TABLE I
SD, VA, AND MF STAND FOR SPHERE DECODING, VITERBI'S ALGORITHM, AND MATCHED FILTER, RESPECTIVELY; r_{stbc} DENOTES THE RATE OF THE ORTHOGONAL ST BLOCK CODE IN [15]. NOTE ALSO THAT [12] HAS BEEN SHOWN AS A MULTICARRIER REPRESENTATIVE, [24] AS A SINGLE-CARRIER ONE (RECALL THAT [24] ALSO SUBSUMES [2], [10], AND [19]), AND DD [5], [14] ARE USED TO REPRESENT THE EXISTING DELAY DIVERSITY SCHEMES THAT HAVE BEEN DEVELOPED FOR $(N_t, N_r) = (2, 1)$

schemes	STM	STF [12]	ZP-only [24]	DD [5]	DD [14]
N_t	$\forall N_t$	$\forall N_t$	$\forall N_t$	2	2
N_r	$\forall N_r$	$\forall N_r$	$\forall N_r$	1	1
decoder	SD	SD	VA	VA	MF
complexity	$\mathcal{O}((N_t(L+1))^{\alpha})$	$\mathcal{O}((L+1)^{\alpha})$	$\mathcal{O}((\lvert\mathcal{A}_s\rvert)^L)$	/	/
G_d	$N_tN_r(L+1)$	$N_tN_r(L+1)$	$N_tN_r(L+1)$	$2(L+1)$	$L+2$
G_c	$\frac{Nd^2_{\min}}{(N+L_{cp})N_t}$	$\frac{Nd^2_{\min}}{(N+L_{cp})N_t}$	$\frac{d^2_{\min}}{N_t}$	/	/
rate (s/s/Hz)	$\frac{N}{N+L_{cp}}$	$\frac{N}{N+L_{cp}}r_{stbc}$	$\frac{N}{N+L_{cp}}r_{stbc}$	$\frac{N}{N+2L+1}$	$\frac{N}{N+L+2}$

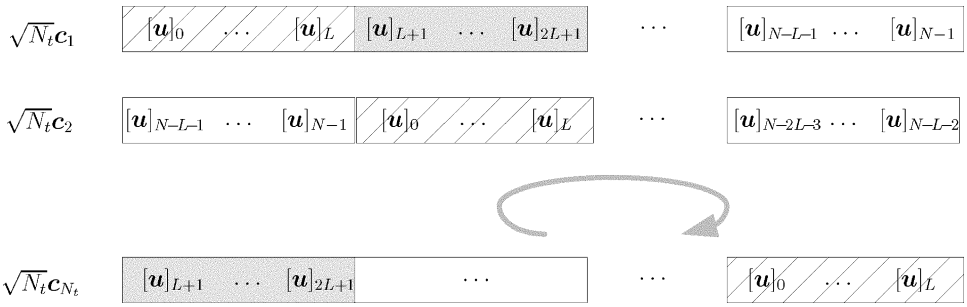

Fig. 4. Circular delay.

$\boldsymbol{\Theta}_{\text{sub}}$ only needs to be greater or equal to $(L+1)$. The reason is that our method renders N_t channels (each with length $L+1$) equivalent to a single channel with length $N_t(L+1)$. The idea is consistent with the one in [12]. In the context of existing ST codes for frequency-selective channels [4], [10], [12], [14], [19], [24], STM offers the following attractive features:

1) STM enables full space-multipath diversity gain $r_h \leq N_tN_r(L+1)$.
2) STM guarantees large coding gains.
3) STM is flexible to strike desirable performance-complexity tradeoffs.
4) Compared with ST block codes, STM suffers no rate loss $\forall N_t$, N_r.
5) Compared with ST trellis codes, STM affords easier code construction and constellation-independent decoding complexity.

More quantitative comparisons of STM with existing alternatives (both single- and multi-carrier ones) are given in Table I.

V. BLOCK CIRCULAR DELAY DIVERSITY INTERPRETATION

In this section, we will reinterpret and modify our DPS-based STM design to gain further insights, as well as establish applicability of STM coding to both multi-carrier and single-carrier systems.

A. Multi-carrier Systems

Recalling $\boldsymbol{\Phi}_\mu$ in (9), it is easy to show using the IFFT matrix definition that

$$\boldsymbol{F}_N^{\mathcal{H}}\boldsymbol{\Phi}_\mu := \begin{bmatrix} \boldsymbol{f}_0^T \\ \vdots \\ \boldsymbol{f}_{N-1}^T \end{bmatrix} \boldsymbol{\Phi}_\mu = \begin{bmatrix} \boldsymbol{f}_{(\mu-1)(L+1)}^T \\ \vdots \\ \boldsymbol{f}_{(\mu-1)(L+1)-1}^T \end{bmatrix} \tag{19}$$

where $\boldsymbol{f}_n^T$ is the nth row of $\boldsymbol{F}_N^{\mathcal{H}}$. Equation (19) shows that left multiplying matrix $\boldsymbol{\Phi}_\mu$ by the IFFT matrix $\boldsymbol{F}_N^{\mathcal{H}}$ is equivalent to permuting the rows of $\boldsymbol{F}_N^{\mathcal{H}}$ circularly. Therefore, there exists an $N \times N$ permutation matrix $\boldsymbol{P}_\mu$ such that

$$\boldsymbol{P}_\mu\boldsymbol{F}_N^{\mathcal{H}} = \boldsymbol{F}_N^{\mathcal{H}}\boldsymbol{\Phi}_\mu, \quad \forall \mu \in [1, N_t] \tag{20}$$

where

$$\boldsymbol{P}_\mu := \begin{bmatrix} \boldsymbol{0} & \boldsymbol{I}_{(\mu-1)(L+1)} \\ \boldsymbol{I}_{N-(\mu-1)(L+1)} & \boldsymbol{0} \end{bmatrix}, \quad \forall \mu \in [1, N_t]. \tag{21}$$

Defining $\tilde{\boldsymbol{u}} := \boldsymbol{F}_N^{\mathcal{H}}\boldsymbol{u}$, and based on the definition of $\boldsymbol{P}_\mu$ in (21), we find that

$$\begin{aligned}\sqrt{N_t}\boldsymbol{c}_\mu &= \boldsymbol{P}_\mu\tilde{\boldsymbol{u}} \\ &= \left[[\tilde{\boldsymbol{u}}]_{(\mu-1)(L+1)} \cdots [\tilde{\boldsymbol{u}}]_N \cdots [\tilde{\boldsymbol{u}}]_{(\mu-1)(L+1)-1}\right]^T. \end{aligned} \tag{22}$$

We infer from (22) that the transmitted block $\boldsymbol{c}_\mu$ on the μth antenna is nothing but a circularly delayed version of the previous ones (see Fig. 4). We summarize this observation as follows.

Property 2: A DPS-based transmission (Fig. 2) is equivalent to a block circular delay diversity (BCDD) transmission (Fig. 5).

Different from the delay diversity designs of [5] and [14], our DPS-based (or equivalently BCDD-based) STM scheme for frequency-selective channels does not sacrifice bandwidth efficiency. Compared with the STM design in Fig. 2, our equivalent model in Fig. 5 has lower complexity because it requires only one IFFT operation (instead of N_t IFFT operations). Further comparisons with [5] and [14] are given in Table I.

B. Single-Carrier Systems

From Fig. 5, we notice that if we do not perform IFFT at the transmitter, i.e., if we eliminate the $\boldsymbol{F}_N^{\mathcal{H}}$ box, we obtain

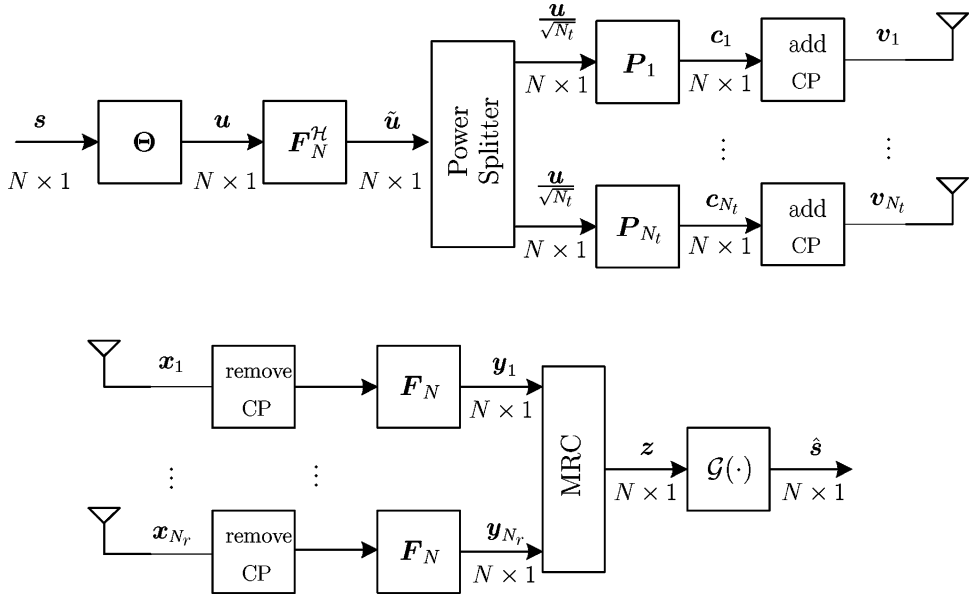

Fig. 5. Discrete-time Tx-Rx model of multi-carrier STM designs.

a single-carrier transmission. This implies that our DPS (or BCDD) scheme is also applicable to single carrier transmissions that are known to be less sensitive to carrier frequency offsets and nonlinear power amplifier effects than their multi-carrier counterparts.

Without going into details, we will summarize the steps for single-carrier systems as follows.

At the transmitter, do the following:

- T1) Given N_t, N_r and L, choose the block size $N > N_t(L+1)$.
- T2) Design the $N \times N$ linear constellation precoder $\boldsymbol{\Theta}$ according to [24].
- T3) Form the precoded vector $\boldsymbol{u} = \boldsymbol{\Theta s}$, and split the power to form $\boldsymbol{u}/\sqrt{N_t}$.
- T4) Apply a circular delay (via $\boldsymbol{P}_\mu$) per antenna to obtain $\boldsymbol{c}_\mu = \boldsymbol{P}_\mu \boldsymbol{u}/\sqrt{N_t}$, $\forall \mu \in [1, N_t]$.
- T5) Insert CP before transmitting each block $\boldsymbol{c}_\mu$.

At the receiver, do the following.

- R1) Remove the CP, and take the FFT of each block.
- R2) Perform MRC of blocks from all the receive antennas, as in (14).
- R3) Implement ML decoding using SD or Viterbi's algorithm for each block, as in (18).

VI. Simulated Performance

Here, we present simulations to test the performance of our STM designs.

Test case 1 (Effects of multipath diversity): In order to appreciate the importance of multipath diversity, we simulate our DPS-based STM design with $N_t = 2$ transmit and $N_r = 1$ receive antennae in the presence of multi-ray channels with different channel orders: $L = 0, 1, 2$. The channel taps are i.i.d. complex Gaussian distributed with zero mean and variance $1/(L+1)$. Quadrature phase shift keying (QPSK) modulation is selected. The subblock size is $N_{\rm sub} = N_t(L+1)$, and the number of subblocks is $N_g = 6$. The information block length is $N = N_{\rm sub}N_g$. Fig. 6 depicts the average bit-error rate (BER) versus SNR. We observe that as L increases, our STM design achieves higher diversity order.

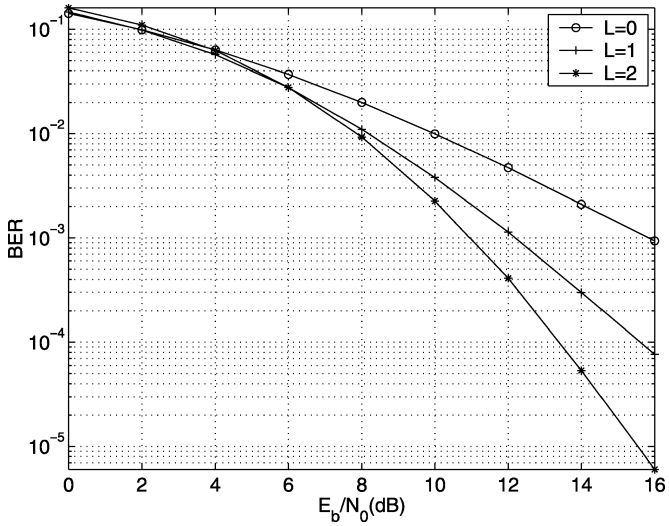

Fig. 6. Multipath diversity effects with increasing channel orders and fixed $(N_t, N_r) = (2, 1)$.

Test case 2 (Diversity-complexity tradeoffs): To tradeoff diversity with complexity, we adjust the group size $N_{\rm sub}$. The parameters and the channel model are the same as in Test case 1, except that we now fix $L = 2$. In this case, $G_d^{\max} = N_t N_r(L+1) = 2 \cdot 1 \cdot 3 = 6$. Fig. 7 confirms that as $N_{\rm sub}$ decreases, the achieved diversity decreases. Since the channel correlation matrix $\boldsymbol{R}_h$ has full rank, the achieved diversity order is $N_{\rm sub}$. Comparing the slopes of BER curves in Figs. 6 and 7 confirms our result. Recall that decoding complexity also decreases as $N_{\rm sub}$ decreases. This shows that when the product $N_t(L+1)$ is large, we can reduce $N_{\rm sub}$ to lower complexity.

Test case 3 (Comparisons with [12] and [24]): In this example, we have $N = 40$, $L_{cp} = L = 2$, $N_r = 1$, and $N_t = 2, 5$. We generate each channel correlation matrix

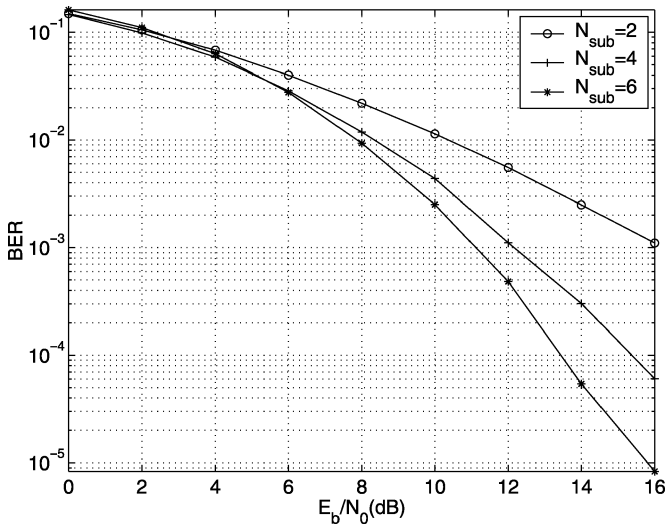

Fig. 7. Performance-complexity tradeoffs.

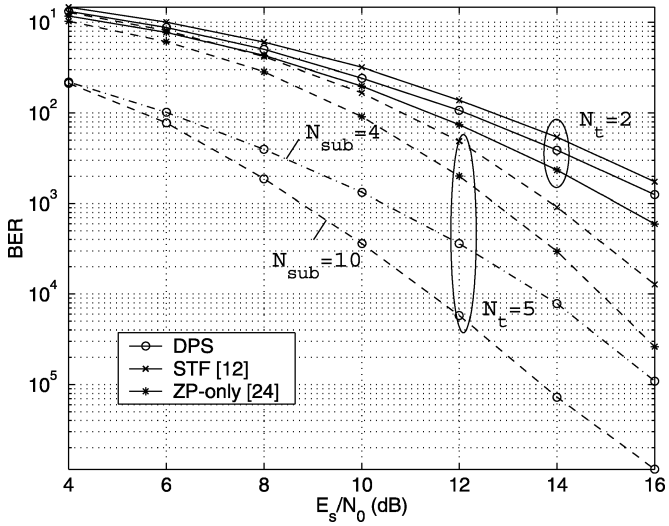

Fig. 8. Comparisons with [12] and [24] (correlated channels).

$E[\boldsymbol{h}^{(\nu,\mu)}(\boldsymbol{h}^{(\nu,\mu)})^{\mathcal{H}}] = \boldsymbol{U}\boldsymbol{\Lambda}\boldsymbol{U}^{\mathcal{H}}$, where $L_e \leq L$ is the "effective" channel order, $\boldsymbol{U}$ is an $(L+1)\times(L_e+1)$ unitary matrix, and $\boldsymbol{\Lambda}$ is an $(L_e+1)\times(L_e+1)$ diagonal matrix. The entries of $\boldsymbol{\Lambda}$ satisfy the realistic exponentially decaying power profile. Here, we select $L_e = 1$. We consider the channels corresponding to different antennas to be independent. Thus, the full diversity order is $G_d = r_h = N_t N_r(L_e+1)$. We generate $\boldsymbol{h}^{(\nu,\mu)} = \bar{\boldsymbol{U}}\boldsymbol{\Lambda}^{\frac{1}{2}}\bar{\boldsymbol{h}}^{(\nu,\mu)}$, where the entries of $\bar{\boldsymbol{h}}^{(\nu,\mu)}$ are i.i.d. with zero mean and unit variance. We select [12] and [24] to represent the multi-carrier and single-carrier ST schemes in the literature, respectively.

When $N_t = 2$, we select QPSK for STM, which is the STF of [12], and the zero-padding (ZP)-only scheme in [24]. For STM and STF, we apply the Sphere-Decoding (SD) algorithm [18] on subblocks of size $N_{\rm sub} = N_t(L_e+1)$ for STM and $N_{\rm sub} = L_e+1$ for STF. To maintain comparable decoding complexity, we implement Viterbi's Algorithm for the ZP-only scheme in [24]. With E_s denoting symbol (s) power, Fig. 8 depicts the BER performance of these three ST codecs. From the slope of the BER curves for $N_r = 1$, we note that all three schemes guarantee the maximum diversity order $G_d^{\max} = N_t N_r(L_e+1) = 4$. Fig. 8 also shows that STM outperforms STF by about 0.8 dB, whereas STF has lower computational complexity. The ZP-only scheme of [24] has the best performance.

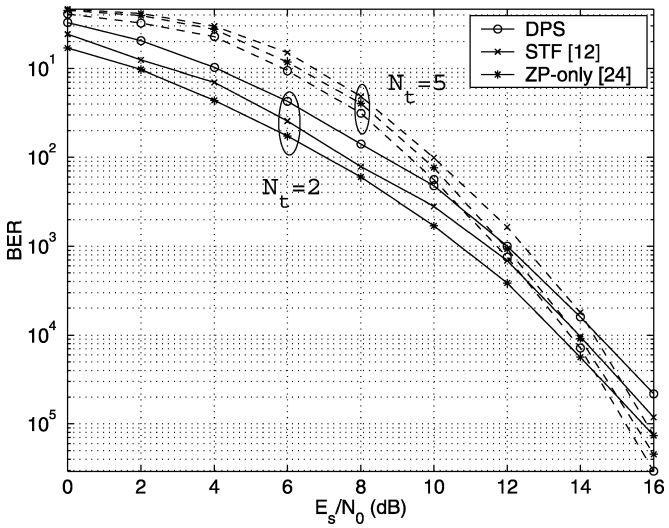

Fig. 9. Comparisons with [12] and [24] (coded case).

However, when $N_t = 5$, to maintain the same transmission rate, we select binary phase shift keying (BPSK) for our STM and QPSK for STF [12] and ZP-only [24], because STF and ZP-only use the ST block code of [17], which has rate 1/2. When we select $N_{\rm sub} = N_t(L_e+1) = 10$ for STM, from Fig. 8, we observe that our STM outperforms both [12] and [24] by about 4 to 5 dB at 10^{-3}. In this case, STM has higher decoding complexity than ZP-only and STF. To lower complexity, we select $N_{\rm sub} = 4$ for STM. In this case, the achievable diversity is only $G_d = 4$. However, even when $N_{\rm sub} = 4$, STM outperforms ZP-only and STF over a large range of SNR values.

Test case 4 (Convolutionally coded designs): In this example, we compare our STM against STF with coded transmissions. We select $N = 40$, $L = 1$, $N_r = 1$, and $N_t = 2$, 5. The channel taps are independent and satisfy an exponentially decaying power profile. Each channel tap is characterized by Jakes' model with mobile speed 3 m/s, carrier frequency 5.2 GHz, and sampling period 4 μs. When $N_t = 2$, we select a rate-1/2 convolutional code with generator [131, 171] and memory 6 for STM, STF, and ZP-only. The depth of the block interleaver is 40. Fig. 9 depicts BER performance of these three schemes, where SNR is defined as the transmitted symbol power over the noise power. When $N_t = 5$, we use the rate-1/2 ST block code of [17] for STF and ZP-only. To maintain the same transmission rate, we select a rate-1/2 convolutional code with 8-QAM for our STM design and a rate-3/4 convolutional code (generator [5, 4, 3, 2; 4, 6, 5, 5; 6,1,4,3] and memory 6) with 16-QAM for STF and ZP-only. From Fig. 9, we observe that i) compared with Test case 3, the same schemes perform worse here because the channels are time-varying; ii) as N_t increases, the diversity order increases; iii) when $N_t = 2$, STF and ZP-only outperform STM by 1 dB; iv) when $N_t = 5$, STM performs better than STF and ZP-only; and v) when we fix the symbol energy, the coding gain depends on the constellation size, which also confirms our result in Proposition 1.

VII. Conclusions

We studied space-time multipath coding for frequency-selective MIMO channels. Novel digital phase sweeping (or block circular delay) designs enable the maximum joint space-multipath diversity and large coding gains. They also afford a low-complexity implementation when working with linearly precoded small-size groups of symbols. Their unique feature is a high rate $(N/(N+L_{cp}))$ symbols/s/Hz) operation, *regardless* of the constellation, and *for any* number of transmit- and receive antennae.[1]

Appendix A
Proof of Proposition 1

Similar to [8], [12], [16], and [24], we will resort to the pairwise error probability (PEP) to design our optimality criteria. Define the PEP $P(\boldsymbol{s}\to\boldsymbol{s}'|\boldsymbol{h}^{(\nu,\mu)},\forall\nu,\mu)$ as the probability that maximum likelihood (ML) decoding of $\boldsymbol{s}$ erroneously decides $\boldsymbol{s}'$ instead of the actually transmitted $\boldsymbol{s}$.

As $\boldsymbol{x}_\nu$ in (3) depends on $\boldsymbol{s}$, we will use ML decoding to detect $\boldsymbol{s}$ from $\{\boldsymbol{x}_\nu\}_{\nu=1}^{N_r}$. Supposing we have estimated the previous and removed the IBI perfectly, the Chernoff bound (conditioned on the $\boldsymbol{h}^{(\nu,\mu)}$'s) yields

$$P\left(\boldsymbol{s}\to\boldsymbol{s}'|\boldsymbol{h}^{(\nu,\mu)},\forall\nu,\mu\right)\le\exp\left(-\frac{d^2(\tilde{\boldsymbol{x}},\tilde{\boldsymbol{x}}')}{4N_0}\right)\tag{23}$$

where $\tilde{\boldsymbol{x}}:=[(\sum_{\mu=1}^{N_t}\boldsymbol{H}^{(1,\mu)}\boldsymbol{v}_\mu)^T,\ldots,(\sum_{\mu=1}^{N_t}\boldsymbol{H}^{(N_r,\mu)}\boldsymbol{v}_\mu)^T]^T$, and the distance in the exponent is

$$d^2(\tilde{\boldsymbol{x}},\tilde{\boldsymbol{x}}')=\sum_{\nu=1}^{N_r}\left\|\sum_{\mu=1}^{N_t}\boldsymbol{H}^{(\nu,\mu)}\boldsymbol{e}_\mu\right\|^2$$

and $\boldsymbol{e}_\mu:=\boldsymbol{v}_\mu-\boldsymbol{v}'_\mu$. Using the commutativity between a Toeplitz matrix and a vector, we can write $\boldsymbol{H}^{(\nu,\mu)}\boldsymbol{e}_\mu=\boldsymbol{E}^{(\mu)}\boldsymbol{h}^{(\nu,\mu)}$, where $\boldsymbol{E}^{(\mu)}$ is a Toeplitz matrix with first column $[\boldsymbol{e}_\mu^T,\boldsymbol{0}^T]^T$. With these definitions, we can rewrite $d^2(\tilde{\boldsymbol{x}},\tilde{\boldsymbol{x}}')$ as $d^2(\tilde{\boldsymbol{x}},\tilde{\boldsymbol{x}}')=\boldsymbol{h}^{\mathcal{H}}\boldsymbol{A}_e\boldsymbol{h}$, where $\boldsymbol{h}$ is defined in (4), and

$$\begin{aligned}\boldsymbol{A}_e&:=\boldsymbol{I}_{N_r}\otimes\left(\boldsymbol{\Phi}_e^{\mathcal{H}}\boldsymbol{\Phi}_e\right),\quad N_rN_t(L+1)\times N_rN_t(L+1)\\ \boldsymbol{\Phi}_e&:=\left[\boldsymbol{E}^{(1)},\ldots,\boldsymbol{E}^{(N_t)}\right],\quad N\times N_t(L+1).\end{aligned}\tag{24}$$

Eigenvalue decomposition of $\boldsymbol{R}_h$ in (4) yields $\boldsymbol{R}_h=\boldsymbol{U}_h\boldsymbol{\Lambda}_h\boldsymbol{U}_h^{\mathcal{H}}$, where $\boldsymbol{\Lambda}_h:=\mathrm{diag}[\sigma_0^2,\ldots,\sigma_{r_h-1}^2]$, and $\boldsymbol{U}_h$ is an $N_tN_r(L+1)\times r_h$ unitary matrix satisfying $\boldsymbol{U}_h^{\mathcal{H}}\boldsymbol{U}_h=\boldsymbol{I}_{r_h}$. Define an $r_h\times 1$ normalized channel vector $\bar{\boldsymbol{h}}$ with entries $\bar{h}_q^{(\nu,\mu)}$ that are i.i.d. Gaussian distributed with zero mean and unit variance. Vectors $\boldsymbol{h}$ and $\boldsymbol{U}_h\boldsymbol{\Lambda}_h^{1/2}\bar{\boldsymbol{h}}$ have identical distributions. Therefore, the PEP remains statistically invariant when one replaces $\boldsymbol{h}$ by $\boldsymbol{U}_h\boldsymbol{\Lambda}_h^{1/2}\bar{\boldsymbol{h}}$. To proceed, let us define the $r_h\times r_h$ matrix

$$\boldsymbol{\Psi}_e:=\left(\boldsymbol{U}_h\boldsymbol{\Lambda}_h^{\frac{1}{2}}\right)^{\mathcal{H}}\boldsymbol{A}_e\boldsymbol{U}_h\boldsymbol{\Lambda}_h^{\frac{1}{2}}.\tag{25}$$

[1]The views and conclusions contained in this document are those of the authors and should not be interpreted as representing the official policies, either expressed or implied, of the Army Research Laboratory or the U.S. Government.

Since $\boldsymbol{\Psi}_e$ is Hermitian, there exists a unitary matrix $\boldsymbol{U}_e$ and a real non-negative definite diagonal matrix $\boldsymbol{\Lambda}_e$ so that $\boldsymbol{U}_e^{\mathcal{H}}\boldsymbol{\Psi}_e\boldsymbol{U}_e=\boldsymbol{\Lambda}_e$. The $r_h\times r_h$ diagonal matrix $\boldsymbol{\Lambda}_e:=\mathrm{diag}[\lambda_0,\ldots,\lambda_{r_h-1}]$ holds on its diagonal the eigenvalues of $\boldsymbol{\Psi}_e$ that satisfy $\lambda_m\ge 0$, $\forall m\in[0,r_h-1]$. The vector $\tilde{\boldsymbol{h}}=\boldsymbol{U}_e\bar{\boldsymbol{h}}$ has the same distribution as $\bar{\boldsymbol{h}}$, because $\boldsymbol{U}_e$ is unitary. Thus, $d^2(\tilde{\boldsymbol{x}},\tilde{\boldsymbol{x}}')$ can be rewritten in terms of the eigenvalues of the matrix $\boldsymbol{\Psi}_e$ as

$$d^2(\tilde{\boldsymbol{x}},\tilde{\boldsymbol{x}}')=\sum_{m=0}^{r_h-1}\lambda_m|\tilde{h}_m|^2.\tag{26}$$

Since we wish our STM coders to be independent of the particular channel realization, it is appropriate to average the PEP over the independent Rayleigh distributed $|\tilde{h}_m|^2$'s. If $r_e:=\mathrm{rank}(\boldsymbol{\Psi}_e)$, then r_e eigenvalues of $\boldsymbol{\Psi}_e$ are nonzero; without loss of generality, we denote these eigenvalues as $\lambda_0\ge\cdots\ge\lambda_{r_e-1}$. At high SNR, the resulting average PEP is bounded as follows [c.f. (23)]:

$$\bar{P}(\boldsymbol{s}\to\boldsymbol{s}')\le\prod_{m=0}^{r_e-1}\left(\frac{\lambda_m}{4N_0}\right)^{-1}=\left(G_{e,c}\frac{1}{4N_0}\right)^{-G_{e,d}}\tag{27}$$

where $G_{e,d}:=r_e$ is the diversity order, and $G_{e,c}:=(\prod_{m=0}^{r_e-1}\lambda_m)^{1/r_e}$ is the coding gain for the error pattern $\boldsymbol{e}:=\boldsymbol{s}-\boldsymbol{s}'$. Accounting for all possible pairwise errors, the diversity and coding gains for our STM multi-antenna systems are defined, respectively, as

$$G_d:=\min_{\forall\boldsymbol{e}\neq\boldsymbol{0}}r_e,\ \text{and}\ G_c:=\min_{\forall\boldsymbol{e}\neq\boldsymbol{0}}G_{c,e}.\tag{28}$$

As the rank of a matrix cannot exceed its dimensionality, checking the dimensionality of $\boldsymbol{\Psi}_e$, we recognize that by appropriately designing our transmission, it is possible to achieve

$$G_d^{\max}=r_h\le N_tN_r(L+1)\tag{29}$$

if and only if the matrix $\boldsymbol{\Psi}_e$ in (25) has full rank r_h, $\forall\boldsymbol{e}\neq\boldsymbol{0}$.

However, it is not easy to express the coding gain G_c in closed form for linearly coded ST systems. However, we can benchmark it, when $\boldsymbol{R}_h$ has full rank $N_rN_t(L+1)$. In addition, it is well known that at reasonably high SNR, the diversity order plays a more important role than the coding gain when it comes to improving the performance in wireless fading channels [16]. Thus, our STM coding will focus on maximizing the diversity order first and then improving the coding gain as much as possible.

Suppose temporarily that $G_d^{\max}$ in (29) has been achieved, i.e., that $\boldsymbol{\Psi}_e$ has full rank $\forall\boldsymbol{e}\neq\boldsymbol{0}$. By (25), we obtain

$$G_c=\min_{\forall\boldsymbol{e}\neq\boldsymbol{0}}\left[\det(\boldsymbol{\Psi}_e)\right]^{\frac{1}{r_h}}=\min_{\forall\boldsymbol{e}\neq\boldsymbol{0}}\left[\det(\boldsymbol{\Lambda}_h)\det(\boldsymbol{A}_e)\right]^{\frac{1}{r_h}}.\tag{30}$$

Furthermore, using the definition of $\boldsymbol{A}_e$ in (24), we find that if $r_h=N_rN_t(L+1)$

$$\begin{aligned}\det(\boldsymbol{A}_e)&=\left(\det\left(\boldsymbol{\Phi}_e^{\mathcal{H}}\boldsymbol{\Phi}_e\right)\right)^{N_r},\quad\text{with}\\ \boldsymbol{\Phi}_e^{\mathcal{H}}\boldsymbol{\Phi}_e&=\left[\boldsymbol{E}^{(1)}\ \cdots\ \boldsymbol{E}^{(N_t)}\right]^{\mathcal{H}}\left[\boldsymbol{E}^{(1)}\ \cdots\ \boldsymbol{E}^{(N_t)}\right]\\ \left(\boldsymbol{E}^{(\mu)}\right)^{\mathcal{H}}\boldsymbol{E}^{(\mu)}&:=\begin{bmatrix}\|\boldsymbol{e}_\mu\|^2 & \lozenge & \lozenge\\ \vdots & \ddots & \vdots\\ \lozenge & \lozenge & \|\boldsymbol{e}_\mu\|^2\end{bmatrix}_{(L+1)\times(L+1)}\end{aligned}$$

where $\Diamond$ stands for terms that are irrelevant at this point, and $\boldsymbol{e}_\mu := \boldsymbol{v}_\mu - \boldsymbol{v}'_\mu$. Based on Hadamard's inequality [7, p. 117], we can upper-bound G_c in (30) as

$$G_c \leq (\det(\boldsymbol{R}_h))^{\frac{1}{r_h}} \min_{\forall \boldsymbol{e} \neq \boldsymbol{0}} \left(\prod_{\mu=1}^{N_t} \|\boldsymbol{e}_\mu\|^2 \right)^{\frac{1}{N_t}}. \tag{31}$$

To maintain a fixed transmit power, we set

$$E\left[\boldsymbol{v}_\mu^{\mathcal{H}} \boldsymbol{v}_\mu\right] = \frac{1}{N_t} E[\boldsymbol{s}^{\mathcal{H}} \boldsymbol{s}] = \frac{N}{N_t}\sigma_s^2, \quad \forall \mu \tag{32}$$

where σ_s^2 is the power per information symbol. Condition (32) dictates equal power per antenna, which is well justified since we assume no channel knowledge at the transmitter. Based on (1), condition (32) is equivalent to

$$\sum_{n=0}^{N-1} \left(\boldsymbol{a}_n^{(\mu)}\right)^{\mathcal{H}} \boldsymbol{a}_n^{(\mu)} + \left(\boldsymbol{b}_n^{(\mu)}\right)^{\mathcal{H}} \boldsymbol{b}_n^{(\mu)} = \frac{N}{N_t}, \quad \forall \mu \in [1, N_t]. \tag{33}$$

Arguing by contradiction, it follows readily from (33) that

$$\min_{\forall p \in [0,P-1]} \left(\sum_{n=0}^{N-1} \left(\left| \left[\boldsymbol{a}_n^{(\mu)}\right]_p \right|^2 + \left| \left[\boldsymbol{b}_n^{(\mu)}\right]_p \right|^2 \right) \right) \leq \frac{N}{PN_t} \leq \frac{1}{N_t}. \tag{34}$$

Now, let $\mathcal{A}_v^{(\mu)}$ be the finite alphabet set for the entries of $\boldsymbol{v}^\mu$. Notice that the left-hand side of (34) is related to the minimum Euclidean distance $\delta_{\min}^{(\mu)}$ among the constellation points in $\mathcal{A}_v^{(\mu)}$. If we let $d_{\min}$ denote the same distance for the points in $\mathcal{A}_s$, we deduce that

$$\begin{aligned} \left(\delta_{\min}^{(\mu)}\right)^2 &= \min_{v,v' \in \mathcal{A}_v^{(\mu)}} |v - v'|^2 \\ &\leq d_{\min}^2 \min_{\forall p \in [0,P-1]} \left(\sum_{n=0}^{N-1} \left(\left| \left[\boldsymbol{a}_n^{(\mu)}\right]_p \right|^2 + \left| \left[\boldsymbol{b}_n^{(\mu)}\right]_p \right|^2 \right) \right) \\ &\leq \frac{1}{N_t} d_{\min}^2, \quad \forall \mu \in [1, N_t] \end{aligned} \tag{35}$$

Based on (35), we can further upper bound G_c in (31) by $G_c^{\max} = (\det(\boldsymbol{R}_h))^{(1/r_h)}(d_{\min}^2/N_t)$. Note that the maximum coding gain $G_c^{\max}$ depends on the underlying constellation through $d_{\min}^2$ and is inversely proportional to the number of transmit antennas N_t because of the power splitting.

REFERENCES

[1] D. Agrawal, V. Tarokh, A. Naguib, and N. Seshadri, "Space-time coded OFDM for high data-rate wireless communication over wideband channels," in *Proc. Veh. Technol. Conf.*, Ottawa, ON, Canada, May 18–21, 1998, pp. 2232–2236.

[2] N. Al-Dhahir, "Single-carrier frequency-domain equalization for space-time block-coded transmissions over frequency-selective fading channels," *IEEE Commun. Lett.*, vol. 5, no. 7, pp. 304–306, Jul. 2001.

[3] H. Bölcskei and A. J. Paulraj, "Space-frequency codes broadband OFDM channels," in *Proc. Wireless Commun. Networking Conf.*, vol. 1, Chicago, IL, Sep. 23–28, 2000, pp. 1–6.

[4] ——, "Space-frequency codes for broadband fading channels," in *Proc. IEEE Int. Symp. Inform. Theory*, Washington, DC, Jun. 2001, p. 219.

[5] D. Gore, S. Sandhu, and A. Paulraj, "Delay diversity code for frequency selective channels," *Electron. Lett.*, vol. 37, no. 20, pp. 1230–1231, Sep. 27, 2001.

[6] A. Hiroike, F. Adachi, and N. Nakajima, "Combined effects of phase sweeping transmitter diversity and channel coding," *IEEE Trans. Veh. Technol.*, vol. 41, pp. 170–176, May 1992.

[7] R. A. Horn and C. R. Johnson, *Topics in Matrix Analysis*. Cambridge, U.K.: Cambridge Univ. Press, 1991.

[8] W.-Y. Kuo and M. P. Fitz, "Design and analysis of transmitter diversity using intentional frequency offset for wireless communications," *IEEE Trans. Veh. Technol.*, vol. 46, no. 4, pp. 871–881, Nov. 1997.

[9] Y. Li, "Simplified channel estimation for OFDM systems with multiple transmit antennas," *IEEE Trans. Wireless Commun.*, vol. 1, no. 1, pp. 67–75, Jan. 2002.

[10] E. Lindskög and A. Paulraj, "A transmit diversity scheme for channels with intersymbol interference," in *Proc. Int. Conf. Commun.*, vol. 1, New Orleans, LA, Jun. 18–22, 2000, pp. 307–311.

[11] Y. Liu, M. P. Fitz, and O. Y. Takeshita, "Space-time codes performance criteria and design for frequency-selective fading channels," in *Proc. Int. Conf. Commun.*, Helsinki, Finland, Jun. 11–15, 2001, pp. 2800–2804.

[12] Z. Liu, Y. Xin, and G. B. Giannakis, "Space-time-frequency coded OFDM over frequency-selective fading channels," *IEEE Trans. Signal Process.*, vol. 50, no. 10, pp. 2465–2476, Oct. 2002.

[13] B. Lu and X. Wang, "Space-time code design in OFDM systems," in *Proc. Global Telecommun. Conf.*, vol. 2, San Francisco, CA, Nov. 27–Dec. 1 2000, pp. 1000–1004.

[14] A. F. Naguib, "On the matched filter bound of transmit diversity techniques," in *Proc. IEEE Int. Conf. Commun.*, vol. 2, Helsinki, Finland, Jun. 11–14, 2001, pp. 596–603.

[15] N. Seshadri and J. H. Winters, "Two signaling schemes for improving the error performance of Frequency-Division Duplex (FDD) transmission systems using transmitter antenna diversity," *Int. J. Wireless Inform. Networks*, pp. 49–60, 1994.

[16] V. Tarokh, N. Seshadri, and A. R. Calderbank, "Space-time codes for high data rate wireless communication: performance criterion and code construction," *IEEE Trans. Inf. Theory*, vol. 44, pp. 744–765, Mar. 1998.

[17] V. Tarokh, H. Jafarkhani, and A. R. Calderbank, "Space-time block codes from orthogonal designs," *IEEE Trans. Inf. Theory*, vol. 45, no. 5, pp. 1456–1467, Jul. 1999.

[18] E. Viterbo and J. Boutros, "A universal lattice code decoder for fading channels," *IEEE Trans. Inf. Theory*, vol. 45, no. 5, pp. 1639–1642, Jul. 1999.

[19] F. W. Vook and T. A. Thomas, "Transmit diversity schemes for broadband mobile communication systems," in *Proc. Veh. Tech. Conf.*, vol. 6, Boston, MA, Sep. 24–28, 2000, pp. 2523–2529.

[20] Z. Wang and G. B. Giannakis, "Wireless multi-carrier communications: Where Fourier meets Shannon," *IEEE Signal Process. Mag.*, vol. 17, no. 3, pp. 29–48, May 2000.

[21] ——, "Complex-field coding for OFDM over fading wireless channels," *IEEE Trans. Inf. Theory*, vol. 49, no. 3, pp. 707–720, Mar. 2003.

[22] A. Wittneben, "A new bandwidth efficient transmit antenna modulation diversity scheme for linear digital modulation," in *Proc. IEEE Int. Conf.Commun.*, vol. 3, Geneva, Switzerland, May 23–26, 1993, pp. 1630–1634.

[23] Y. Xin, Z. Wang, and G. B. Giannakis, "Space-time diversity systems based on linear constellation precoding," *IEEE Trans. Wireless Commun.*, vol. 2, no. 2, pp. 294–309, Mar. 2003.

[24] S. Zhou and G. B. Giannakis, "Single-carrier space-time block coded transmissions over frequency-selective fading channels," *IEEE Trans. Inf. Theory*, vol. 49, no. 1, pp. 164–179, Jan. 2003.

Xiaoli Ma (M'03) received the B.S. degree in automatic control from Tsinghua University, Beijing, China, in 1998 and the M.Sc. and Ph.D. degrees in electrical engineering from the University of Virginia, Charlottesville, in 1999 and the University of Minnesota, Minneapolis, MN, in 2003, respectively.

Since August 2003, she has been an assistant professor with the Department of Electrical and Computer Engineering, Auburn University, Auburn, AL. Her research interests include transmitter and receiver diversity techniques for wireless fading channels, communications over time- and frequency-selective channels, complex-field and space-time coding, channel estimation and equalization algorithms, carrier frequency synchronization for OFDM systems, and wireless sensor networks.

Georgios B. Giannakis (F'97) received the Diploma in electrical engineering from the National Technical University of Athens, Athens, Greece, in 1981 and the M.Sc. degree in electrical engineering in 1983, the MSc. degree in mathematics in 1986, and the Ph.D. degree in electrical engineering in 1986, all from the University of Southern California (USC), Los Angeles.

After lecturing for one year at USC, he joined the University of Virginia, Charlottesville, in 1987, where he became a Professor of electrical engineering in 1997. Since 1999, he has been a professor with the Department of Electrical and Computer Engineering, University of Minnesota, Minneapolis, where he now holds an ADC Chair in Wireless Telecommunications. His general interests span the areas of communications and signal processing, estimation and detection theory, time-series analysis, and system identification—subjects on which he has published more than 160 journal papers, 300 conference papers, and two edited books. Current research focuses on transmitter and receiver diversity techniques for single- and multiuser fading communication channels, complex-field and space-time coding, multi-carrier, ultrawide band wireless communication systems, cross-layer designs, and distributed sensor networks.

Dr. Giannakis is the (co-) recipient of four best paper awards from the IEEE Signal Processing (SP) Society in 1992, 1998, 2000, and 2001. He also received the Society's Technical Achievement Award in 2000. He served as Editor in Chief for the IEEE SIGNAL PROCESSING LETTERS, as Associate Editor for the IEEE TRANSACTIONS ON SIGNAL PROCESSING and the IEEE SIGNAL PROCESSING LETTERS, as secretary of the SP Conference Board, as member of the SP Publications Board, as member and vice-chair of the Statistical Signal and Array Processing Technical Committee, as chair of the SP for Communications Technical Committee, and as a member of the IEEE Fellows Election Committee. He is currently a member of the the IEEE-SP Society's Board of Governors, the Editorial Board for the PROCEEDINGS OF THE IEEE, and chairs the steering committee of the IEEE TRANSACTIONS ON WIRELESS COMMUNICATIONS.